A Comparative Study of the Thermal Evaluation of the PTC System in Saharan Areas

Hocine Mahcene Abdelkader[1], Salah Tlili[2*], Abdelmadjid Kaddour[3], Mohamed Said Nedjimi[4], Mohammed Abdelkader Belalem[5], Medjadji Nassira[6], Medjahed Driss Meddah[7], Mohamed Lakhdar Belfar[8]

[1,2]Univ. Ouargla, Fac. Mathematics and Material Sciences, Lab. Development Of New And RenewableEnergies In Arid And Saharan Zones Laboratory (LARENZA), 30000, Ouargla, Algeria
[3]Unité de Recherche Appliquéeen Energies Renouvelables, URAER, Centre de Développement desEnergies Renouvelables, CDER, 47133, Ghardaïa, Algeria
[4,8]Univ. Ouargla, Fac. Mathematics and Material Sciences, Lab. Valorisation and Promotion of Saharan Resources Laboratory (VPRS), 30000, Ouargla, Algeria.
[5]Sciences and environmental research laboratory, department of materials sciences, faculty of sciences and technology, University of Tamanghasset, Algeria
[6]Electrical Engineering Department, University Center Salhi Ahmed Naama, Naama 45000, Algeria
[7]Mechanical Engineering Department, University Center Salhi Ahmed Naama, Naama 45000, Algeria.

***E-mail:** tlilisalah2007@gmail.com

Received: September 05, 2023, Revised: November 03, 2023, Accepted: December 08, 2023, Published: December 17, 2023

Abstract:

Tamanrasset and Adrar regions were chosen to study the water heating performance using a parabolic cylindrical solar concentrator, and calculations were used for this. But before that, we examined the evolution of the total daily intensities of direct solar radiation, as well as its relationship to the duration of insolation and the maximum air temperature during the year, with the aim of choosing the days when the values of these amounts are the lowest in each region. We found that smaller quantities occur over several days, and due to the great similarity of these quantities, we settled for two days, the first being the winter solstice and the second being the seventh day of the year. During which the evolution of the intensity of direct solar radiation, the air temperature, the water temperature at the outlet of the solar center, the flow of absorbed thermal energy, instantaneous or total, were monitored, and finally the total thermal efficiency.

We noticed that the shape of the evolution of the first four is generally parabola-shaped, while the evolution of the last two differs from it and is similar, regardless of the school day and its region. Comparing the two regions, the values of most quantities are the highest in the Adrar region, with a close deviation at maximum values and a significant deviation at sunset. This difference is of the order of 200 W/m^2, 3-5 °C, 8-9 °C, 1-1.5 kW, 30-40 MW, and 50-60%, depending on the previous arrangement of the quantities studied. The intensity of direct solar radiation is excluded from the maximum value because it is the highest in the Tamanrasset region, with a slight difference estimated at 8 W/m^2. Comparing the two days of the study, the values of the seventh day of January are the highest, both for the intensity of direct solar radiation (2-18 W/m^2), and for the thermal

energy flow absorbed, whether instantaneous (0.15-0.01 kW) or total (4 MW). While it is lower for all air temperatures (2-3°C), outlet temperature (0.5-1.5°C) and efficiency (15%).
Keywords: solar radiation, air temperature, linear parabolic solar concentrator, outlet temperature, absorbed thermal energy, thermal efficiency.

Tob Regul Sci. ™ 2023 ;9(2): 1896-1912
DOI: doi.org/10.18001/TRS.9.2.121

Introduction

Most countries around the world aim to reduce greenhouse gas (GHG) emissions as their main objective. As a sustainable solution, in order to replace combustible energies, renewable energies are needed, and for precision, the solar deposit is large in certain countries. [1,2].

Parabolic solar collector (PTC) technology is one of the most frequently used types of CSP systems worldwide, with more affordable system design and optimization.

The basic parts of a PTC are an evacuated tube and a linear parabolic reflector. The reflector is made by bending a reflecting material into a parabolic shape and the evacuated tube is located in the focus line of this parabola. The main idea of this technology is the reflection of the solar beam radiation from the parabolic reflector towards to the evacuated tube in order to heat the working fluid. The general efficiency improvements and the cost reduction of PTC systems are essential factors for the further development of CSP systems worldwide [3,4].

Khudair et al. 2022, simulated the change in direction of the sun's position relative to the (PTC), and they improved the efficiency of the (PTC) by knowing the effect of the angle of incidence of the solar rays.[5]

Lamrani et al. 2018, found that the large effect on the outlet temperature of the HTF and the use of synthetic oil is dominated by the length of the receiver tube, in addition they revealed that the maximum value of 76% of the thermal efficiency of the solar collector is completed during the summer. [2]

Tzivanidis et al. 2015, used a commercial software Solidworks in order to simulate the efficiency performance under different operating conditions. [6]

Mokheimer et al. 2014, found that the reduction by different mechanical works of specific cost of a PTC field for about 46% and 48% at 10 hectares and about 72% and 75% at 160 hectares, respectively, compared to that at 2.8 hectares. [7]

Kaddour et al. 2023, studied the thermal performance of the absorber tube using ANSYS, by the choiseof the solar parabolic trough collector with air in the annulus space. [8]

Daoui et al. 2023, evaluated the performance of the PTC concentrator in the two arid Algerian sites of Ghardaia and El Oued, respectively. [9]

Mouaky et al. 2019, simulated and validated a PTC model using experimental data from a PTC test loop, installed at the Green Energy Park research facility. [10]

Wirz et al. 2014, assessed the potential improvements of the efficiency of PTC systems by component idealizations and secondary optics, and they identified the most promising avenues for further research and development. [11]

Kouche et al. 2022, carried out a numerical simulation in order to obtain the approximate solution to the nonlinear system of partial differential equations that characterize the parabolic trough heat collector element using a numerical algorithm which combines the finite difference method for the semi

discretization in time (semi-implicit predictor–corrector method) with the finite element method (FEM) for the space discretization. [12]

Abdulhamed et al. 2018, emphasized geometrical analysis, thermal mathematicaldesign, thermal efficiency, applications, and experimental setups of the collector/receiver of a Parabolic Trough Solar Powered Collector in terms of temperature, heat flux, heat loss, and ambient conditions. [13]

Conrado et al. 2017, proposed new methodologies that efficiently measure the thermal performance of a Parabolic Trough Solar Collector and they reduced the costs of these collectors. [14]

Chargui et al. 2021, found in the new PTC design, the useful daily energy gain increased by 33% and 15%, and the system thermal efficiency increased by 8.9% and 5.8% in summer and winter, respectively, in comparison to the case of mono-axial orientation without a glass envelope. [15]

Fan et al. 2018, investigated the applicability of the solar heating system in different geographical regions with different meteorological conditions, of which parabolic trough solar collectors (PTCs) were operated with the absorption heat pumps (AHP) and oil/water heat exchanger (OWHE) at medium and low operating temperature respectively. [16]

Zou et al. 2015, found that the thermal efficiency of the proposed PTC reached about 67% even under the condition of solar radiation of less than 310 W/m2, indicating that the PTC could collect solar radiation efficiently. [17]

The main context of this paper: a comparative study between the efficiencies of a cylindrical solar center with a linear parabola, these efficiencies being represented by the water outlet temperature, the instantaneous and total thermal energy, and the total yield in two different regions of the south of the Algeria, located approximately in a close longitude. This was done after comparing the characteristics of two regions in terms of total direct solar radiation intensities, the ratio of this total to insolation time, and absolute temperatures to choose the study days corresponding to the lowest of these values

PTC system design

The studied system is presented in the present figure1:

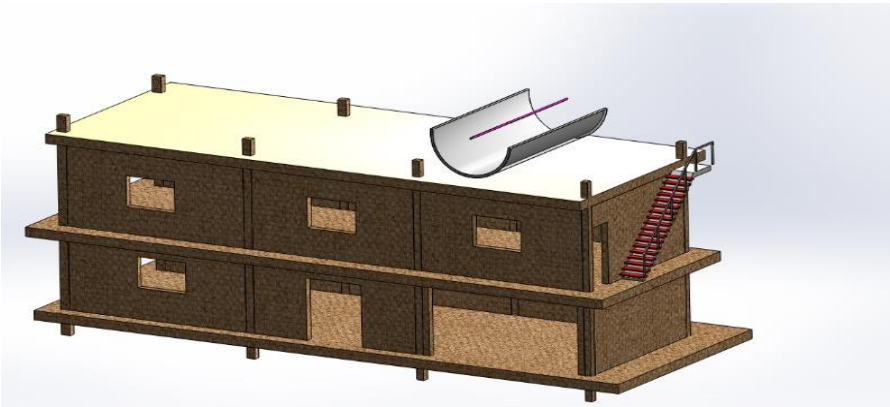

Fig. 1. The studied PTC system

Methodology:

By following the steps briefly included in the diagram shown in Figure (2) below, the objectives of this study can be achieved, as it is noted that this diagram is divided as follows:

1. The entries, which are:

A: The figures for longitude (°) A, latitude (°) M, and height H above sea level, that is, the three topographical values. The day number of the month N_{jm} and the month number of the year N_m (day number of the year) are used to ensure the daily change of the output.

Table 1: Astronomical location values for the study area

	Adrar	**Tamanrasset**
Altitude	229	1402
Latitude	20,504	22,47
Longitude	-13,046	5,31

B: Tables of the highest and lowest absolute temperatures for each month and for each region are listed in Table 2 below.

Table 2: Maximum and minimum monthly temperature values for the two study areas

	Adrar		**Tamanrasset**	
	Tmax	**Tmin**	**Tmax**	**Tmin**
JANUARY	24,01	12,11	19,00	03,00
FBRUARY	28,25	15,52	21,00	05,00
MARCH	30,39	18,50	25,00	08,00
APRIL	42,11	27,47	30,00	13,00
MAY	43,25	30,08	33,00	17,00
JUNE	44,66	34,44	35,00	21,00
JULY	46,72	36,49	35,00	21,00
AUGUST	44,94	36,24	34,00	21,00
SEPTEMBER	42,27	32,54	32,00	18,00
OCTOBER	35,98	25,89	29,00	15,00
NOVEMBER	30,76	17,79	25,00	10,00
DECEMBER	23,84	11,57	21,00	06,00

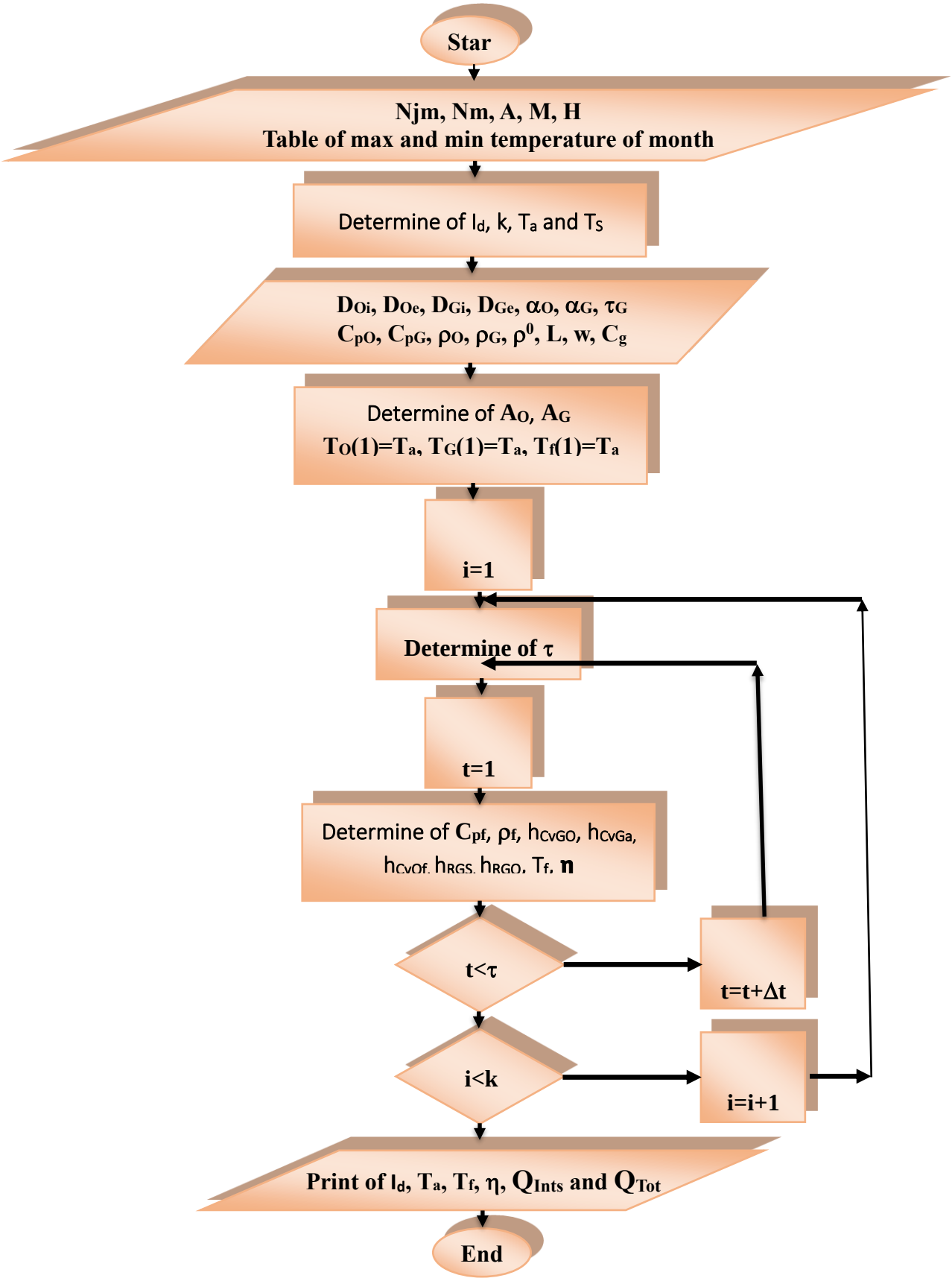

Fig. 2. Flowchart of the calculation of our methodology

C- Values representing the properties of the cylindrical, linear, and parabolic heliocentric used with length L (5m) and Width w (3m), they are respectively related to the water-carrying tube and the glass cover wrapped around it, (0.019 m) D_{Oi}, (0.049 m) D_{Gi} internal diameters. (0.02 m) D_{Oe}, (0.05 m) D_{Ge}, outer diameters. (0.97) α_O, (0.5) α_G Absorption. (385 j/kg.K) C_{pO}, (835 j/kg.K) C_{pG} Heat capacity. (8940 kg/m^3) ρ_O, (2530 kg/m^3) ρ_G Density of the material from which the glass tube and cover are made. In addition to, (0.935) τ_G glass envelope transmittance, (0.935) ρ^0 Reflection coefficient and finally (40) C_g Geometric focus of radiation.

2: Arithmetic operations: where

A. The intensity of direct solar radiation (W/m^2) is calculated from one of the numerous models among which the works are presented: Capderou, 1987, [18] Kasten, 1996, [19] Louche et al., 1986 [20]; Trabelsi and Masmoudi, [21]2011 The absolute temperature of the study area Ta and the sky temperature TS (K) are also calculated, respectively, using the relationships of Reicosky et al., 1989 [22]; Belghit et al., 1997 [23]; and Garcia-Valladares and Velazquez, 2009 [24] All these calculations are carried out after determining that k(s) is the local time, which allows calculating k(s) the daytime isolation time, by which the number of repetitions throughout the day can be measured.

B: Calculate the cross section of each water-carrying tube and glass cover, respectively (m2). Assigning the absolute zone temperature value (K) Ta at sunrise as the starting temperature value for the water, the water-conducting pipe, and the glass cover

C- Relying mainly on a set of hypotheses based on thermodynamics and heat balance theories for heat transfer in the three parts that make up the center, to simplify and organize the equations presented in the work of Daoui et al. (2023 [9] which are repeated at each instant t of the isolation time (in this study we took t = 1 s), we can find:

Cpf is the specific heat capacity of water (W/m2).

hCvGO is the heat transfer coefficient by convection between the glass cover and the absorbent element (W/K.m).

- h_{CvGa} is the heat transfer coefficient by convection between the glass cover and the environment (W/K.m).
- -h_{CvOf} is the heat transfer coefficient by convection between the absorbent element and the fluid (W/K.m).
- h_{RGS} is the heat transfer coefficient by radiation between the glass envelope and the sky (W/K.m).
- heat transfer coefficient by h_{RGO} radiation between the glass cover and the absorbent element (W/K.m).
- T_f Temperature of the working fluid (K).
- η Total thermal efficiency or central efficiency (%).

.This repetition only occurs within a time(s) of the amount of water passing through the entire pipeline, which must be determined in advance.

3- Outputs: Not all coefficients calculated above are required as outputs, as we will only look at the values of each of: The intensity of direct solar radiation, the absolute temperature of the area, the outlet temperature of the water and total thermal efficiency. In addition to other parameters whose calculations are simple and of great importance in our study, they are among the important results, which are: Q_{Ints} of instantaneous thermal energy gained, Q_{Tot} of total instantaneous thermal energy gained (W).

Note: Study days are determined based on the results of the previous two steps. The following days can theoretically be found for each study area:

- The day when the total intensity of direct solar radiation is highest compared to that of other days. This total is calculated as follows:

$$SI = \sum_{i=1}^{n} I_d(i)$$

- The day when the ratio between the total intensity of solar radiation and the rest time is the highest compared to that of other days, which is calculated as follows:

$$SIt = \frac{SI}{t}$$

Today the minimum value of air temperature is the highest compared to other days.

III. Presentation and discussion of results:

III-1: Determination of study days:

In order to better determine the days of study in this work, it was necessary to examine the evolution of the total daily intensity of direct solar radiation, the relationship of this total to the duration of insolation, and the temperature of the highest air temperature during the year in both study areas. These changes are shown in figures (5, 4, 3).

Just by looking at the figures, we can see that there is great consistency in the evolution of the shapes of these coefficients throughout the year. This good convergence may be due to the proximity of the latitude between the two regions, because it appears from Table 1 that the difference is estimated at 1.97. But it is certain that the difference in air temperature can be due to the difference in altitude above sea level, since in Table 1, we notice that the Tamanrasset region is more than 1,200 m higher than the Adrar region. From figure (3), we notice that the values of the total intensity of daily direct solar radiation only increase, strongly and in a somewhat linear manner, from December 22 for the Tamanrasset region and from December 21 for the Tamanrasset region of the same month for the Adrar region until approximately April 25. However, the total daily intensity of direct solar radiation reaches its highest value in the Tamanrasset region on May 28 and is highest on the 19th of the same month in the Adrar region a month later. After these two days, the values of this amount begin to decrease, but slowly, until approximately the last day of August in both study areas. After this day, the decrease continues, but strongly, until the two days from which the increase began, these two days being those where the value of this amount is the lowest in both regions. This difference could be due to the difference in altitude above sea level, since in Table 1, we notice that the Tamanrasset region is more than 1,200 m higher than the Adrar region.

As for figure (4), we see that the evolution of the values of the ratio between the intensities of solar radiation and the duration of insolation during the year in the two study areas is increasing in two periods and decreasing in the other two. Increased periods: the first phase increases rapidly in an almost linear manner and begins on December 21 in the Tamanrasset region and the 20th of the same month in the Adrar region, ending on April 19 and the 15th of the same month. same month, while maintaining the same previous ranking of the region, these are the two days where this amount is the highest of the year. The second period begins around the beginning of July and ends around the beginning of September in both regions, but the increase is much slower there. Between these two periods, a decrease occurs in the value of this amount. In the first period, this decrease is very slow, in total contrast to the second period. Thus, the twenty-first of December in the Tamanrasset region and the twentieth of the same month in the Adrar region provide the lowest values of this amount throughout the year.

From figure (5), which represents the evolution of the values of the maximum air temperature, it is clear that this value is constant every month and is the same in the second column of table (2). The values are always the highest in the Adrar region, but with a gap that always varies. It can be said that this difference is very small in winter, with the exception of its increase in February. In spring, the difference decreases

despite its high value, while in summer it is almost equal, with a clear decrease in autumn. The highest values of this amount appear in the month of June (or July) in the Tamanrasset region and in July in the Adrar region, while the lowest value appears in the month of January, exactly on the seventh day from the first region, and in the month of December, exactly on the second day, and twenty in the second district. It is these last two days that are important in this study because their values are 19 and 24 °C, respectively, as shown in Table 3.

Table (3) shows that the values of both the total intensities and their relationship to the duration of insolation are very close to the point of being equal between the first and second of December in the Tamanrasset region, while in the region of Adrar, the values of these two values are almost equal between December 20 and 21, like last month. We also believe that their values are always the twentieth of the same month, so December twenty-second, designated for the winter solstice, can be chosen as the most important day of study. It is also possible to neglect the difference in the values of these two amounts in addition to the air temperature between the seventh day of January and the twenty-fifth day of December, especially since the difference between these degrees is not only five degrees. Finally, we can simply use January 7 and December 22 as the best choices to study the results of using a cylindrical parabolic solar concentrator to heat water in the two regions.

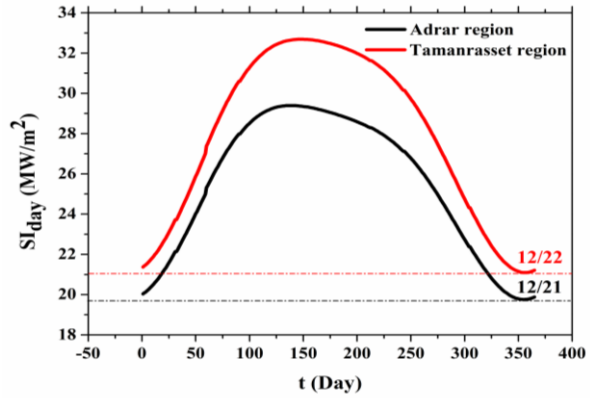

Fig. 3. Daily changes in total direct solar radiation intensities over the course of a year in the two study areas.

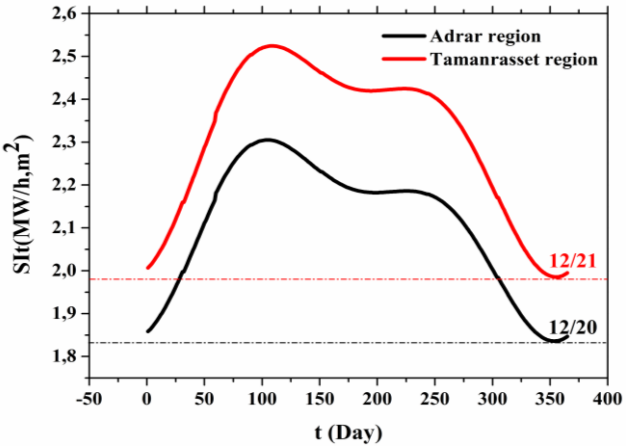

Fig. 4. Daily changes in the ratio between the total intensities of solar radiation and the duration of insolation during the year in the two study areas

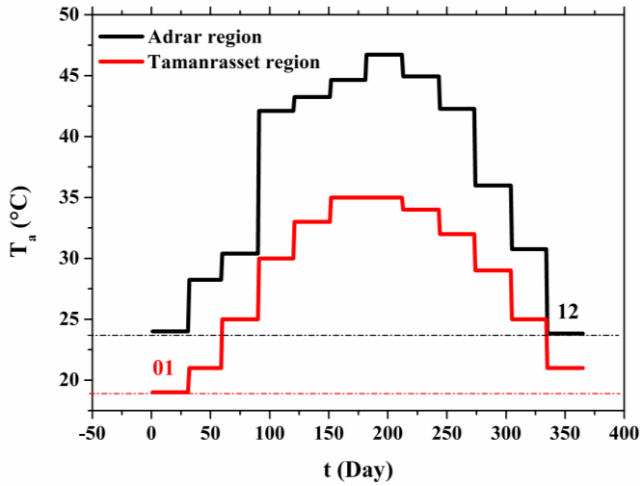

Fig. 5.: Daily changes in maximum air temperature over the course of a year in the two study areas.

Table 3: Values of the characteristics of the days corresponding to the lowest sum of the daily values of the intensity of direct solar radiation, to the lowest ratio of this sum to the duration of insolation, and to the maximum temperature of the lowest air in both fields of study

		Nj	M	J	I(W/m²)	t(h)	SI(MW/m²)	SI/t(MW/h,m²)	Tamb(°C)
Adrar	The minimum of Total daily radiation (W/m²)	355	12	21	833,02	10,76	19,76	1,84	24
	The minimum of Average daily hourly radiation (W/m².h)	354	12	20	832,89	10,76	19,76	1,84	24
	The minimum of Tamax (°C)	359	12	25	834,23	10,76	19,77	1,84	24
Tamanrasset	The minimum of Total daily radiation (W/m²)	356	12	22	841,25	10,62	21,1	1,99	21
	The minimum of Average daily hourly radiation (W/m².h)	355	12	21	841,17	10,63	21,1	1,99	21
	The minimum of Tamax (°C)	7	1	7	859,56	10,69	21,67	2,03	19

III-2 Study of the Evolution of Climate Variables:

III-2-1 Study of the Evolution of the Intensity of Direct Solar Radiation:

Figure 6 shows the evolution of the intensity of direct solar radiation during the day, both within the days and in the study areas. The most important moments and radiation intensities are also recorded in the first two lines, from which it is clear that:

The first sunrise occurs on December 22, shortly after six thirty a.m. This time, it's more than three minutes earlier than January 7 in the same area. The same timetable is about ten minutes ahead of its counterpart in the Adrar region on the same day and about eight minutes the other day.

The evolution of this radiation takes the form of an approximate parabola depending on its arrival time, as shown in Table 4. It appears from the values in this table that in the same area, the difference between the arrival times of the two study days is less than three minutes, while on the same day, this difference between the two study areas is less than fifty minutes. The strange thing is that the period between sunrise and the start of radiation, especially in the Adrar region, lasts about two hours, and it is also shorter on June 7. In the Tamanrasset region, this duration does not exceed forty minutes, and it is almost equal between the two study days.

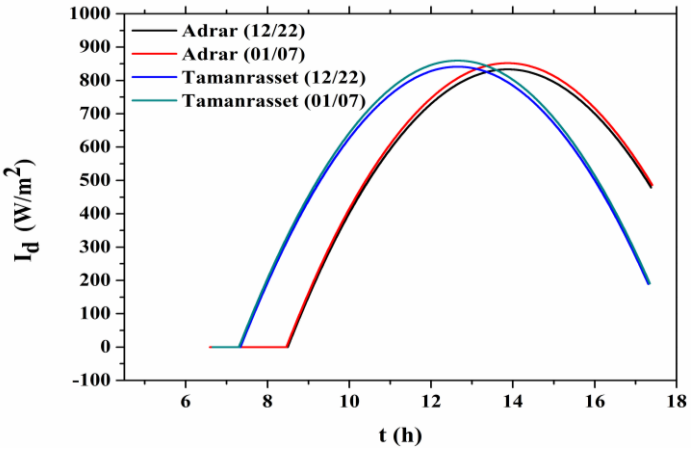

Fig. 6. Instantaneous evolution of direct solar radiation over the two days and the two study areas.

The time when the radiation reaches its maximum is the same during the two days of study in the same area, since it is more than an hour and ten minutes in the Tamanrasset region. The radiation intensity here on January 7 is about 18 W/m² higher than that on December 22, i.e., the study area, while it is higher than its counterpart in the region of the Adrar of approximately 8 W/m², that is to say. on the day of the study.

It appears that there is a large difference in radiation intensity between the two regions, whatever the day of the study, since its value in the Adrar region exceeds 100 W/m2, more than double that of its value in the Tamanrasset region. The difference between the two study days is approximately 7 W/m² and 2 W/m², respectively, in the regions of Adrar and Tamanrasset, because its value on December 22 is lower than its value on January 7.

The values of solar radiation intensity in the Tamanrasset region are higher than in the Adrar region from the beginning of its arrival until shortly after one in the afternoon, while at this time the values of these intensities are equal. Before this time, the gap decreases very slowly, especially before noon, but after 1 p.m., the situation is completely reversed since the gap increases slowly after 3 p.m.

The interpretation of this element has been detailed in order to confirm the results obtained when determining the two days of the study, and on the other hand, to not repeat certain values, such as the arrival times of the radiation and the sunset time.

III-2-2 Study of the evolution of absolute air temperature:

The change in air temperature over the two study days in both regions is shown in Figure 7 which confirms what was mentioned above when choosing the two study days. It is clear that the values of this degree are higher than the rest of the values of January 7 in the Adrar region, while they are lower than the values of the same day in the Tamanrasset region, and its values are higher on 22 in the Adrar region than in the

Tamanrasset region. This change takes the form of a parabola, and its peak is at two o'clock in the afternoon, regardless of the day or the study area.

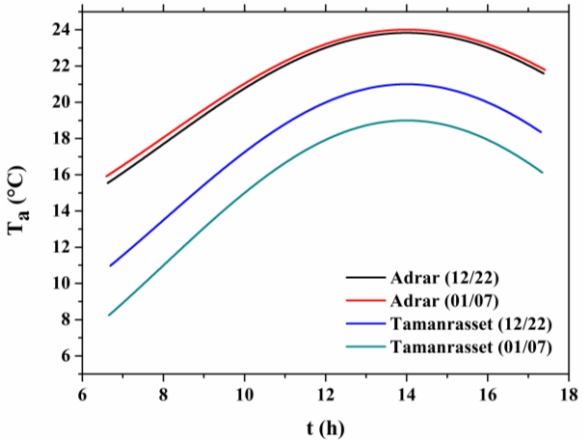

Fig. 7. Instantaneous change in air temperature over the two days and the two study areas.

From the third line of table (4), it is clear that the difference in air temperature between the two study days in the Tamanrasset region is almost constant compared to the case of the Adrar region, but its value in the first region is much higher. But in reality, it is a difference decreasing until the peak and increasing thereafter in the two regions: its values are estimated at 2.73 °C, 0.36 °C at sunrise, 2 °C, 1.17°C at peak, and 2.27 °C, 0.20 °C at sunset, depending on the layout of the two regions. The difference between its values in the two study areas is 7.66 °C, 5.76 °C at sunrise, 5.01 °C, 2.84 °C at the summit, and 5.67 °C, 3.24°C at sunset on January 7 and December 2, right away.

III-3 Study of the evolution of solar center yields:

III-3-1 Study of the evolution of the water outlet temperature:

In figure 8, the change in water temperature leaving the solar center is depicted throughout the study days and in both regions, showing that this change resembles the shape of the change in the intensity of the radiation because it takes the form of a parabola. But the order of values largely corresponds to the change in air temperature, which means that it also has a large effect. Especially in the period between sunrise and the moment of direct solar radiation, which was assumed from the beginning because this temperature is equal to the air temperature,

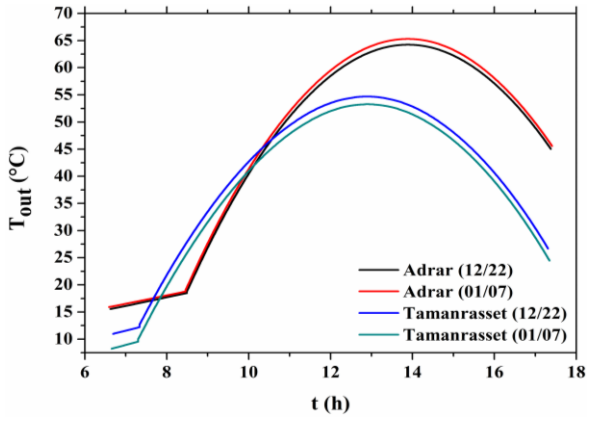

Fig. 8. Instantaneous evolution of the water temperature at the outlet of the solar center on the two days and the two study areas.

According to the values in the fourth row of table (4), when the reading comes, the difference between the values: A temperature is 0.46 degrees Celsius, and a temperature is 0.29 degrees Celsius. The temperature is 9.23 degrees Celsius. Then allow the temperature to cool down to 8.48 degrees Celsius. Temperatures peaked at the same time in the Adrar region during the daily survey, while workers reached them on the 22nd and thirty minutes later than on January 7. Water temperatures are 1.41 °C, 1.41 °C, and 1.06°C in the Adrar region, while the difference between the two study areas is estimated at 10.03°C. Temperature of water: 0.03 °C, 9.56°C Water temperature of 0.03°C in December. At sunset, considering the same results for the days and regions studied, the difference is 1.41°C to 1.06°C. The water temperature is 10.03°C to 9.56°C.

From figure 8, we always see that the values of this outlet temperature are identical in the two regions at two times, regardless of the two days of the study. The first of these is after seven thirty, while the second is around ten.

III-3-2 Study of the Evolution of Instantaneous Thermal Energy Absorption:

Figure 9 represents the flow of instantaneous thermal energy absorbed by the water throughout the day, on both days of the study and in the two regions. The most important results are recorded in the fifth row of Table 4, where:

From this figure, it is clear that the order of their values does not remain constant in the same order as occurs when the air temperature changes (see Figure 7). This means that air temperature has no effect on this quantity. But the form of this change corresponds well to the variation in the intensity of direct solar radiation. Their values are non-existent until the radiation has yet arrived because the outlet temperature is the same as the inlet temperature, which is equal to the air temperature. This agreement is in many respects mentioned above, except at the time of the superiority of values in the Adrar region, which begins around ten thirty.

According to table 4, the temperature reaches its maximum at the same time in both regions during the two days of the study, while its arrival in the Tamanrasset region is approximately one hour and thirteen minutes earlier than in the Adrar region. In corn, the difference between the two study regions is estimated at 1.40 kW on the seventh day of January and 1.34 kW on December 22, while the difference between the two study days was estimated at 0.12 kW in the Tamanrasset region and 0.18 kW in the Adrar region. At sunset, taking into account the same arrangement of days and study areas, the difference between the two study days is estimated to be 3.22 kW and 3.16 kW, while the difference between the two study areas is estimated at 0.01 kW and 0.07 kW.

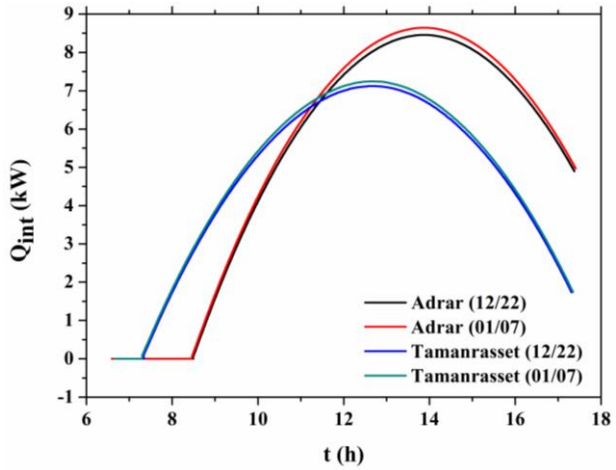

Fig. 9. Instantaneous changes in the instantaneous energy absorbed by the solar center on the two days and the two study areas

.

III-3-3 Study of the evolution of the total thermal energy absorbed:

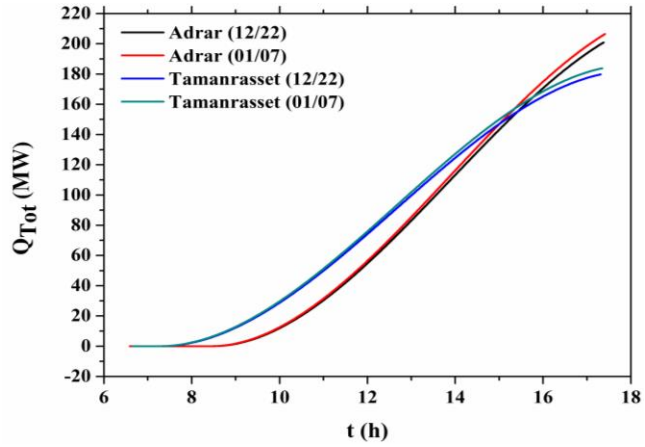

Fig. 10. Instantaneous evolution of the total energy of the solar center over the two days and the two study areas.

The evolution of the total thermal energy flux absorbed during the day on the two days of the study and its regions is described in figure 10. The flow of this energy increases from the moment of arrival of solar radiation, which is before nine and after two in the afternoon in the Tamanrasset region, and before ten and after four in the region of Adrar, where between these two hours the increase is somewhat linear. The values of this flow are identical at the beginning, and over time, the difference between the two study days begins to appear more and more. Where do we finally give values that are still the highest on January 7.

Table (4): The most important values of the calculation results.

		Adrar region		Tamanrasset region	
		22-12	07-01	22-12	07-01
Time during the day	At sunrise	6 h 32 m 12 s	6 h 35 m 24 s	6 h 41 m 24 s	6 h 39 m 36 s
	Beginning of radiation	8 h 29 m 24 s	8 h 27 m 36 s	7 h 20 m 24 s	7 h 18 m 00 s
	At sunset	17 h 22 m 48 s	17 h 24 m 36 s	17 h 18 m 36 s	17 h 21 m 00 s
Intensity of direct solar radiation (W/m²)	At the peak	833.22 at 13 h 52 m 12 s	851.83 at 13 h 52 m 12 s	841.25 at 12 h 39 m 00 s	859.56 at 12 h 39 m 00 s
	At sunset	478.82	485.79	188,88	190.83
Ambient temperature (°C)	At sunrise	15.54	15.92	10.97	8.24
	At the peak	23.84 at 14 h 00 m 00 s	24.01 at 14 h 00 m 00 s	21 at 14 h 00 m 00 s	19 at 14 h 00 m 00 s
	At sunset	21.59	21.79	18.35	16.12
Outlet temperature(°C)	Beginning of radiation	18.49	18.78	10.01	9.55
	At the peak	64.24 at 13 h 53 m 24 s	65.30 at 13 h 53 m 24 s	54.68 at 12 h 53 m 24 s	53.27 at 12 h 54 m 00 s
	At sunset	45.03	45.58	26.67	24.48
Instantaneous absorbed heat energy (kW)	At the peak	8.46 at 13 h 52 m 12 s	8.64 at 13 h 52 m 12 s	7.12 at 12 h 39 m 36 s	7.24 at 12 h 39 m 36 s
	At sunset	4.90	4.97	1.74	1.75
Total absorbed heat energy (MW)		200.96	206.49	179.77	183.83
Total thermal yield (%)		81.44	81.42	56.86	56.61

According to Table 4, they are higher by 4 MW in the Tamanrasset region and higher by 5.53 MW in the region of 'Adrar. On the other hand, after the arrival of solar radiation in the Tamanrasset region until ten o'clock, the values of the flow of this energy in this region are higher with an increasing gap, and after this time they remain higher, but with a decreasing gap, until shortly after three in the afternoon. From this time on, the values of this flow in the Adrar region become the highest, with an ever-increasing gap.

III-3-4 Study of the evolution of the total thermal efficiency:

It is clear from figure (11) that, whatever the day and the region of the study, the evolution of the total thermal efficiency during the day corresponds to the evolution of the flow of total thermal energy absorbed. It also appears that there is a correspondence between its values on the two days of study, despite the fact that they are spaced two weeks apart in each region, which means that this return is not linked to the day of study, despite the long period of difference between them. The linear increase begins after eight and nine hours, respectively, in the Tamanrasset and Adrar regions and ends around three and four hours, respectively. This yield is higher at the beginning and after the arrival of the radiation in the Tamanrasset region until half past noon, where its values start to become higher in the Adrar region. After this time, the difference increases until the end of the day, while before it increases depending on the moment of arrival of solar radiation until the tenth tribe, where it begins to decrease. The final values of this yield are recorded in Table 4, where the lowest value was found in the Tanmarast region on January 7 and is estimated at 56.61%. Its value increases by 0.25% on January 22 in the same region, while its value increases by 24.81% and 24.83%, according to the previous arrangement of the two school days in the Adrar region.

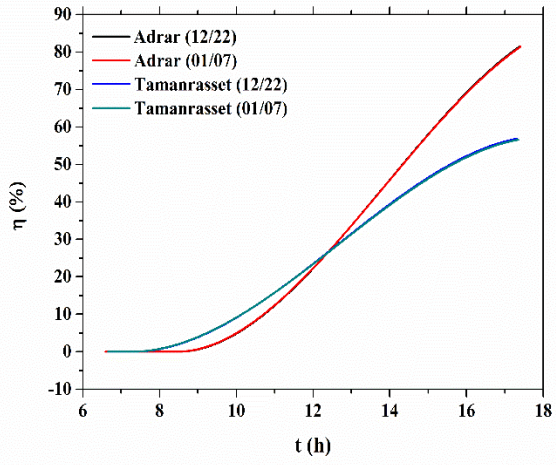

Fig. 11. Instantaneous evolution of the total thermal efficiency over the two days and the two study areas.

Conclusion

Through the results of this work, we can achieve:

The annual variations in the total intensity of direct solar radiation, its relationship to insolation duration, and air temperature appear identical in the two study areas, with a slight difference between them resulting from the difference in longitude, particularly in the study area. last amount resulting from the difference in elevation above the Earth's surface.

The study days were chosen as January 7 and December 22, after specifying broader choices that represent the lowest values of the previous three amounts. This choice does not bring a significant addition because the variation is not significant, so the two days mentioned above may be sufficient. The shape of the parabola dominates most of the quantities studied, with the exception of the total flux of absorbed thermal energy and the total thermal efficiency. Especially based on the timing of the arrival of direct solar radiation, both for the intensity of direct solar radiation and for the two outputs of the cylindrical parabolic solar center, represented by the output temperature and the amount of instantaneous thermal energy absorbed by the water.

Air temperature affects the outlet temperature values, particularly the arrangement and position of these values, but it does not affect the flow of instantaneous thermal energy absorbed by the water. The total thermal efficiency at the start of the day is equal because it is not very affected by the study days; their duration is close.

The results in both regions between the two selected study days are mostly close, as the difference in all cases is negligible and not significant. But it is clear that there is a big difference between the two regions.

This study may be incomplete in many respects, but several lines of research can be proposed, the most important of which are:

- It is possible to adopt other parameters to determine school days.

- It is possible to work on the basis of experimental values for both solar radiation intensity and air temperature because experimental values are often more precise. It is certain that solar radiation is affected by many factors, such as cloudiness, dust, etc. Air temperature is also affected by several factors, including wind speed, direction, etc.

It is possible to carry out completely experimental work, although this is difficult, especially when carrying out solar monitoring using such concentrators.

The study can be generalized throughout the year to reach the values at any time of the year, the minimum having been chosen here in the expectation of better results on other days.

References

[1] The E.E. and S.C. and the C. of the R. Commission Staff Working Document accompanying the Communication from the Commission to the European Parliament, the Council, Second Strategic Energy Review : Energy sources, production costs and performance of technologies for power generation, heating and transport, 744 (2008).

[2] Lamrani, B., Khouya, A., Zeghmati, B., &Draoui, A. (2018). Mathematical modeling and numerical simulation of a parabolic trough collector: A case study in thermal engineering. *Thermal Science and Engineering Progress*, *8*, 47-54.

[3] Price, H., Lu¨ pfert, E., Kearney, D., Zarza, E., Cohen, G., Gee, R., & Mahoney, R. (2002). Advances in parabolic trough solar power technology. *J. Sol. Energy Eng.*, *124*(2), 109-125.

[4] Ouagued, M., Khellaf, A., &Loukarfi, L. (2013). Estimation of the temperature, heat gain and heat loss by solar parabolic trough collector under Algerian climate using different thermal oils. *Energy Conversion and management*, *75*, 191-201.

[5] Khudair, Y. Y., & Hasan, A. B. (2022, August). Optical characteristics of simulated design of parabolic trough solar concentrator. In AIP Conference Proceedings (Vol. 2437, No. 1). AIP Publishing.

[6] Tzivanidis, C., Bellos, E., Korres, D., Antonopoulos, K. A., & Mitsopoulos, G. (2015). Thermal and optical efficiency investigation of a parabolic trough collector. *Case Studies in Thermal Engineering*, *6*, 226-237.

[7] Mokheimer, E. M., Dabwan, Y. N., Habib, M. A., Said, S. A., & Al-Sulaiman, F. A. (2014). Techno-economic performance analysis of parabolic trough collector in Dhahran, Saudi Arabia. *Energy conversion and management*, *86*, 622-633.

[8] Kaddour, A., Belgasim, B., Agagna, B., Behar, O., Achouri, A., Nedjimi, M. S., Tlili & Daoui, H. (2023). A review of tools dedicated to the modeling and simulation of concentrating solar systems. *NeuroQuantology*, *21*(6), 1630-1651.

[9] H. Daoui, S. Tlili, A. Kaddour, Y. Menni, L. Benmebrouk, M. Said. Nedjimi, (2023). Thermal Assessment of the PTC System in Arid Algerian Regions. *Tobacco Regulatory Science (TRS)*, 4056-4073.

[10] Mouaky, A., Merrouni, A. A., &Laadel, N. E. (2019). Simulation and experimental validation of a parabolic trough plant for solar thermal applications under the semi-arid climate conditions. *Solar Energy*, *194*, 969-985.

[11] Wirz, M., Petit, J., Haselbacher, A., & Steinfeld, A. (2014). Potential improvements in the optical and thermal efficiencies of parabolic trough concentrators. *Solar Energy*, *107*, 398-414.

[12] El Kouche, A., & Gallego, F. O. (2022). Modeling and numerical simulation of a parabolic trough collector using an HTF with temperature dependent physical properties. *Mathematics and Computers in Simulation*, *192*, 430-451.

[13] Abdulhamed, A. J., Adam, N. M., Ab-Kadir, M. Z. A., &Hairuddin, A. A. (2018). Review of solar parabolic-trough collector geometrical and thermal analyses, performance, and applications. *Renewable and Sustainable Energy Reviews*, *91*, 822-831.

[14] Conrado, L. S., Rodriguez-Pulido, A., & Calderón, G. (2017). Thermal performance of parabolic trough solar collectors. *Renewable and Sustainable Energy Reviews*, *67*, 1345-1359.

[15] Chargui, R., Tashtoush, B., & Awani, S. (2022). Experimental study and performance testing of a novel parabolic trough collector. *International Journal of Energy Research*, *46*(2), 1518-1537.

[16] Fan, M., Liang, H., You, S., Zhang, H., Yin, B., & Wu, X. (2018). Applicability analysis of the solar heating system with parabolic trough solar collectors in different regions of China. *Applied energy*, *221*, 100-111.

[17] Zou, B., Dong, J., Yao, Y., & Jiang, Y. (2016). An experimental investigation on a small-sized parabolic trough solar collector for water heating in cold areas. *applied energy*, *163*, 396-407.

[18] Capderou, M. (1987). Atlas Solaire de l'Algérie, modèlesthéoriques et expérimentaux. Vol. 1, T1, Office des Publications Universitaires, Algérie.

[19] Kasten, F. (1996). The Linke turbidity factor based on improved values of the integral Rayleigh optical thickness. Solar energy, 56(3), 239-244.

[20] Louche, A., Peri, G., & Iqbal, M. (1986). An analysis of Linke turbidity factor. Solar energy, 37(6), 393-396.

[21] Trabelsi, A., & Masmoudi, M. (2011). An investigation of atmospheric turbidity over Kerkennah Island in Tunisia. Atmospheric Research, 101(1-2), 22-30.

[22] Belghit, A., Belahmidi, M., Bennis, A., Boutaleb, B. C., & Benet, S. (1997). Etude numérique d'un séchoirsolairefonctionnanten convection forcée. Revue générale de thermique, 36(11), 837-850.

[23] Reicosky, D. C., Winkelman, L. J., Baker, J. M., & Baker, D. G. (1989). Accuracy of hourly air temperatures calculated from daily minima and maxima. Agricultural and Forest Meteorology, 46(3), 193-209.

[24] García-Valladares, O., & Velázquez, N. (2009). Numerical simulation of parabolic trough solar collector: Improvement using counter flow concentric circular heat exchangers. International journal of heat and mass transfer, 52(3-4), 597-609.